



Article

Prediction of Drivers' Red-Light Running Behaviour in Connected Vehicle Environments Using Deep Recurrent Neural Networks

Md Mostafizur Rahman Komol^{1,2}, Mohammed Elhenawy^{3,*} , Jack Pinnow⁴, Mahmoud Masoud⁵, Andry Rakotonirainy³, Sebastien Glaser³ , Merle Wood⁴ and David Alderson⁴

- ¹ QUT Centre for Robotics, School of Electrical Engineering and Robotics, Queensland University of Technology, Brisbane 4000, Australia; m.komol@qut.edu.au
- ² Data61 Robotics and Autonomous System Group, Commonwealth Scientific and Industrial Research Organisation (CSIRO), Brisbane 4069, Australia
- ³ Centre for Accident Research and Road Safety-Queensland, Queensland University of Technology, Brisbane 4000, Australia; r.andry@qut.edu.au (A.R.); sebastien.glaser@qut.edu.au (S.G.)
- ⁴ Department of Transport and Main Road (Queensland), Brisbane 4000, Australia; jack.z.pinnow@tmr.qld.gov.au (J.P.); merle.y.wood@tmr.qld.gov.au (M.W.); david.d.alderon@tmr.qld.gov.au (D.A.)
- ⁵ Department of Information Systems & Operations Management, Business School, King Fahd University of Petroleum and Minerals, Dhahran 31261, Saudi Arabia; mahmoud.masoud@kfupm.edu.sa
- * Correspondence: mohammed.elhenawy@qut.edu.au

Abstract: Red-light running at signalised intersections poses a significant safety risk, necessitating advanced predictive technologies to predict red-light violation behaviour, especially for advanced red-light warning (ARLW) systems. This research leverages Long Short-Term Memory (LSTM) and Gated Recurrent Unit (GRU) models to forecast the red-light running and stopping behaviours of drivers in connected vehicles. We utilised data from the Ipswich Connected Vehicle Pilot (ICVP) in Queensland, Australia, which gathered naturalistic driving data from 355 connected vehicles at 29 signalised intersections. These vehicles broadcast Cooperative Awareness Messages (CAM) within the Cooperative Intelligent Transport Systems (C-ITS), providing kinematic inputs such as vehicle speed, speed limits, longitudinal and lateral accelerations, and yaw rate. These variables were monitored at 100-millisecond intervals for durations from 1 to 4 s before reaching various distances from the stop line. Our results indicate that the LSTM model outperforms the GRU in predicting both red-light running and stopping behaviours with high accuracy. However, the pre-trained GRU model performs better in predicting red-light running specifically, making it valuable in applications requiring early violation prediction. Implementing these models can enhance red-light violation countermeasures, such as dynamic all-red extension (DARE), decreasing the likelihood of severe collisions and enhancing road users' safety.

Keywords: cooperative awareness message; connected vehicle; intelligent transportation system; long short-term memory; gated recurrent unit; red-light running prediction



Citation: Komol, M.M.R.; Elhenawy, M.; Pinnow, J.; Masoud, M.; Rakotonirainy, A.; Glaser, S.; Wood, M.; Alderson, D. Prediction of Drivers' Red-Light Running Behaviour in Connected Vehicle Environments Using Deep Recurrent Neural Networks. *Mach. Learn. Knowl. Extr.* **2024**, *6*, 2855–2875. <https://doi.org/10.3390/make6040136>

Academic Editor: Weiping Ding

Received: 30 October 2024

Revised: 25 November 2024

Accepted: 4 December 2024

Published: 11 December 2024



Copyright: © 2024 by the authors. Licensee MDPI, Basel, Switzerland. This article is an open access article distributed under the terms and conditions of the Creative Commons Attribution (CC BY) license (<https://creativecommons.org/licenses/by/4.0/>).

1. Introduction

Worldwide, roughly 1.3 million people are killed every year in road traffic accidents, according to a recent study. In addition, between 20 and 50 million people suffer life-threatening injuries as a result of motor-vehicle-related accidents [1,2]. When it comes to traffic fatalities, the worldwide average is frighteningly high, with 18.2 deaths per 100,000 people [1,3,4], and road intersections account for 43% of all road accidents and 23% of deadly collisions [5]. In 2021, red-light running contributed to fatal accidents resulting in the loss of 1109 lives in the USA [6]. Numerous factors contribute to signalised intersection

crashes, including failure to break quickly at a red light, miscalculated turning angles and distances of other automobiles, and purposefully running a red light [7].

Red-light running behaviour was described by Qian and Dong [8] as a vehicle approaching an intersection after a red light appeared. To find the essential parameters inside the prediction models, it is vital to first understand the psychology underlying red-light running. Red-light running can be associated with a driver's misjudgement at the start of yellow, in which the driver puts himself in a situation that necessitates rapid and decisive action as they approach the intersection. For example, a dilemma zone is an area just before an intersection when the driver must make a split-second choice.

Red-light running at signalised crossings can result in a variety of collisions. Rear-end [9] and right-angle collisions are the two most prevalent collision types caused by red-light violation. As soon as the driver of the lead car decides to suddenly stop at the yellow phase, a rear-end collision can occur. The most common damage from rear-end crashes is whiplash. For right-angle collisions, the red signal is activated to halt vehicle movement in any direction of the intersection, and the perpendicular direction of the intersection is given a green signal to allow vehicles to pass through in a perpendicular manner to the stopped route. However, if a vehicle disregards the red signal and enters the intersection, it enters the conflict zone illegally. At the same time, the perpendicular side of the intersection is signalled green, allowing vehicles approaching at a right angle to also enter the conflict zone, resulting in collisions between vehicles running a red light and those with a green signal. Right-angle accidents are more likely to result in severe injuries due to the dissipation of more kinetic energy. A schematic diagram of red-light violation and right-angle collision is shown in Figure 1.

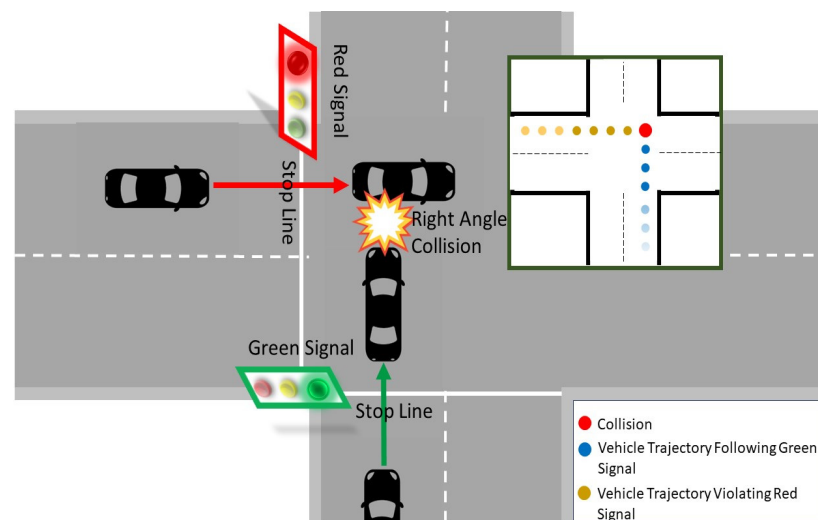


Figure 1. Red-light running traffic violation and right-angle collision [10].

In Figure 1, the green vehicle violated the red signal and ran the red-light, causing a right-angle collision with the orange vehicle in the conflict zone. Drivers' red-light running behaviour can be divided into two categories: (1) passive and (2) deliberate factors. Drivers' unintentional judgments induced by insensitivity and surrounding circumstances are known as passive factors. Driving inexperience, age, weather, road geometry, and blocked vision are all possible causes. Intentional considerations refer to a driver's deliberate decision to practise risky driving behaviour. Aggressive driving, peer pressure, and speeding to save time are shown to be the most common types of traffic rule violations like red-light running, all of which contribute to collisions [11–13].

There have been some solutions to target reducing red-light running. These solutions are cost-effective and, more significantly, minimise the number of crashes, injuries, and fatalities. The dynamic all-red extension (DARE) system is intended to prevent collisions during red-light running breaches. The implementation of the all-red extension technology

ensures that the red signal is activated in all directions at the intersection whenever a potential red-light violation is predicted. This extension delays the activation of the green signal for vehicles waiting at the right-angle direction. This formula significantly enhances road safety by preventing potentially fatal traffic collisions. However, it also imposes hefty traffic fines on drivers who violate traffic rules by running a red light. Consequently, the all-red extension system plays a crucial role in improving road safety. The DARE system is further enhanced to be more cost-effective by dynamically measuring the extension of the red signal activation time for right-angle vehicles based on the time required for the red-light runner to pass through the intersection's conflict zone. Furthermore, the incorporation of the DARE system with connected vehicle technology offers a more precise prevention of red-light violations. Through wireless communication between vehicles and road infrastructure, connected vehicle technology facilitates easy tracking of vehicle kinematic information and GPS positions using embedded devices. This eliminates the need for external cameras, and road signals can operate dynamically by activating an all-red signal in response to any detected red-light violation incidents [14–18]. Similar to the DARE system, Hold the Red (HTR) uses radar technology to track vehicles approaching intersections up to 150 m from the stop line. When it anticipates a red-light violation during the all-red phase, HTR extends the opposing red lights, potentially reducing red-light running crashes by 33.47% with minimal traffic delays [19]. For the DARE and HTR systems, early prediction of drivers' intention to violate red signals is a crucial step for intersection signal management and prevents the likelihood of collisions between red-light runners and right-angle vehicles. Alternatively, early prediction of red-light running can help distracted or drug- or alcohol-influenced drivers to be drawn to react to a warning and prevent traffic violations or collisions. However, no previous research exists on predicting drivers' red-light running behaviour in a C-ITS environment using deep RNN collecting data from a broad field operation test of connected vehicles. In our recently published research on drivers' movement prediction at intersections in a connected vehicle environment [20], it was found that vehicles, intending to turn in the intersection, gradually slow down while approaching the intersection and their turning behaviours change with time. A successful prediction of drivers' intended movements at intersections was measured using recurrent neural networks: Long Short-Term Memory (LSTM) and Gated Recurrent Unit (GRU) models considering different traffic monitoring times at different traffic warning distances before the stop line [20]. So, our hypothesis is that using recurrent neural networks for predicting drivers' red-light running and stopping behaviours will ensure a successful prediction performance considering that drivers who intend to stop at red signals will gradually slow down when approaching the intersection stop-line rather than the drivers who run through the intersection conflict zone violating the red signal.

In this research, we considered connected vehicle kinematic information as input for using recurrent neural networks: we used LSTM and GRU to predict driver red-light running and stopping behaviour at signalised intersections in the connected vehicle environment. This research used the connected vehicle kinematic data from Australia's largest field operation test (FOT): Ipswich Connected Vehicle Pilot project, Australia [21]. The project undergoes the field operation test with 355 connected vehicles at 29 intersections, communicating and broadcasting cooperative awareness messages (CAMs) in cooperative intelligent transport systems (C-ITS). Information regarding the experimental design of the Queensland ICVP project is available within the summary report titled "Ipswich Connected Vehicle Pilot Safety Evaluation [21]. From our research experiment, we found a very limited dataset sample (40 red-light running incidents only) that violated the red signal in the naturalistic environment. It was challenging to obtain a successful model performance using a neural network with such limited dataset samples. Our second hypothesis is that transferring the weights of a fully pre-trained model to initialise our recurrent neural networks (LSTM and GRU networks) will ensure robust performance with such limited dataset samples for predicting drivers' red-light running behaviour. So, we used the transfer

learning technique to train our recurrent neural network models where we considered drivers' movement prediction models (taken from our previous research [20]) as pre-trained models. Moreover, the rising number of accidents and infractions at red lights, especially those caused by drivers disobeying stop signals, emphasises the necessity for an improved predictive system in traffic management. Improper traffic management systems are not able to predict drivers' behaviour before they reach the stop line, which results in ineffective traffic signal timing and delayed reactions to possible threats. The ability to successfully reduce the risks associated with red-light running is limited by this gap in predictive power, which frequently leads to a reactive approach rather than a preventative one. Therefore, in order to accurately predict driver actions before they approach a red light, a reliable prediction model that makes use of several monitoring windows and distances before the stop line is urgently needed.

The contribution of this research is given below:

- Adopting deep RNN: LSTM and GRU to predict drivers' red-light running and stopping behaviour with 355 connected vehicles' kinematic information data at 29 intersections. To the best of our knowledge, this is the first study that investigates red-light violation prediction using deep neural networks in a connected environment based on data collected in a large-scale field operation test. This aspect sets our study apart from previous research. Our study is also the first of its kind conducted in the Australian driving environment. This context adds significant value to the literature and enhances the relevance of our findings.
- Adopted transfer learning technique to achieve robust performance given the inherent scanty dataset sample limitation in red-light running prediction and effectively overcomes this challenge.
- Performance comparison between LSTM and GRU models and evaluating the most efficient models with different traffic monitoring times for drivers' red-light running and stopping behaviour prediction at different warning distances from the stop line. The potential of this predictive capacity can greatly improve traffic safety by enabling the timely implementation of precautionary actions, such as issuing connected vehicle alerts, optimising signal timing, and extending all-red signal phases adaptively.
- Identifying suitable models for balanced prediction of red-light running and stopping behaviour and identifying a hard constraint prediction model for red-light violation where prediction of red-light violation is the highest priority above stopping behaviour prediction.

2. Literature Review

Existing research on red-light running behaviour prediction uses statistical approaches and shallow machine learning approaches like Random Forrest and Support Vector Machine [3,14,22–24]. The potential of the Bayesian Network has been studied extensively, for example, by Chen et al. [25]. Through a hybrid logit–Bayesian network technique, they describe how to formulate driving behaviour in intersections with phone usage distraction. A 96.3% accuracy result was achieved by predicting vehicle trajectory and platoon location. For the data collection, radar sensors were employed. Additionally, it contains SVM (linear) and non-linear SVM (non-linear), Random Forest, and Logistic Regression models. In the study by Jahangiri et al. [26], they analysed vehicle movement patterns and created two models. One of them was a Support Vector Machine (SVM) with a Gaussian kernel, achieving an accuracy of 97.9%, while the other was a Random Forest (RF) model with 500 trees and the Gini criterion, resulting in an accuracy of 93.6%. They incorporated video data along with vehicle trajectories and signals. Additionally, Gates et al. [27] developed a Nested Logit model. Jahangiri et al. [28] utilised the same variables for Random-Forest-based analysis and included epidemiology and distraction as additional variables. The work of Li et al. [18] developed a red-light violation prevention system by harnessing Artificial Neural Networks (ANNs) and simulation data containing vehicle trajectory information. The ANNs demonstrated a reasonable training time and exhibited a prediction

accuracy rate exceeding 80%. In other studies, Pugh and Park [22] delved into an extensive analysis of vehicle trajectory, encompassing epidemiological factors, distractions, dilemma zone characteristics, and changes in pedal direction using an ANN model in conjunction with experimental data and video recordings. Their model achieved an accuracy rate of nearly 82%. Nonetheless, it is worth noting that these studies were constrained by limited experimental resources, such as restricted experiment field coverage or a shortage of available naturalistic data.

Ren et al. [29] conducted research on 9-month red-light running events extracted from high-resolution traffic data collected by loop detectors from three signalised intersections to identify the factors that significantly affect red-light running behaviours. Their research findings indicate that the rare event logistic regression model outperformed the standard logistic regression model by a substantial margin, achieving an accuracy of 77.3%. Importantly, it is worth mentioning that their proposed method for predicting red-light running relies solely on data collected from a solitary advance loop detector positioned 400 feet away from the stop-bar intersection. Hurwitz et al. [30] introduced a probabilistic model with a reliability of roughly 90%. They tested their red-light running predictors by validating them with real-world data from an intersection. The findings suggest that for a functioning DARE (Driver Assistance and Red Light Enforcement) system, the current vehicle detection systems, specifically those equipped with at least two inductive loop detectors (ILDs)—the advance loop closest to the stop bar and the leading presence loop—can offer a satisfactory prediction of red-light running incidents. Additionally, Radar Trajectory Data and an associated algorithm may be employed to detect individuals who run red lights. Zaheri and Abbas [31] developed a discriminant analysis algorithm that has a precision of 96%. The algorithm was supported by radar data with a signal phase, a detector, and video data from a camera.

The prediction of red-light running is a critical element of the dynamic all-red extension (DARE) approach, which has lately gained interest as a non-traditional intersection collision avoidance strategy. Zhang et al. [32] developed an offline data analysis method for determining the parameters needed for predicting red-light running incidents. In order to put this method into practice, they constructed a 2D normal model that predicts a vehicle's stop-and-go behaviour, incorporating improved detector speeds and the following distance to other vehicles. Unlike traditional prediction models that aim to minimise average errors, their approach specifically addresses two types of errors: false alarms (false positives) and missed reports (false negatives). Remarkably, the algorithm achieved effective detections ranging from around 70% to over 80%. However, DARE's effectiveness is limited to a specific subset of precisely timed red-light runners. For instance, it can address situations where vehicles narrowly miss the yellow light and are caught by the fixed red clearance signal. But once a different signal group transitions to green, adhering to DARE's red-light enforcement is no longer feasible.

Zyner et al. [33] demonstrated that recurrent neural networks effectively predict driver intentions at unsignalised intersections, significantly enhancing autonomous vehicle safety by providing a 1.3 s prediction window before potential conflicts. Zyner et al. [34] utilised recurrent neural networks to enhance the prediction of driver intentions and trajectories at unsignalised intersections, significantly advancing the capability of autonomous vehicles to handle dynamic and complex urban traffic scenarios effectively. Lee [35] demonstrated that the Extreme Gradient Boosting model enhanced with Shapley Additive Explanations (SHAPs) significantly improves traffic speed predictions on urban roads by identifying and incorporating highly influential links, offering a robust solution for complex urban traffic management and planning. Ren et al. [29] utilised high-resolution traffic data from loop detectors at three signalised intersections to identify factors influencing red-light running (RLR) behaviours. The study revealed that factors such as occupancy time, used yellow time, and adjacent lane vehicle movements are critical for predicting RLR. Importantly, a rare event logistic regression model was developed, demonstrating superior performance over standard logistic regression models for predicting RLR, leveraging data

from commonly used loop detectors. This research underscores the potential for enhancing intersection safety through real-time data application. Min et al. [36] demonstrated the effectiveness of deep multimodal learning for traffic speed estimation, leveraging dedicated short-range communication and vehicle detection system data, achieving high accuracy and robustness during peak hours and weekends. Kwak and Lee [37] utilised explainable artificial intelligence (XAI) to demonstrate the significant impact of road transport systems on groundwater quality in Texas, identifying key parameters like pH and aluminium influenced by traffic attributes within a 50 m distance and 100 m well depth.

To the best of our knowledge, no research was found on naturalistic red-light running data from a large-scale cooperative intelligent transportation system (C-ITS) field test like ICVP to predict drivers' intended red-light running in intersections considering the change in vehicle kinematic information in time sequence. Unlike other technologies, connected vehicles are not constrained by proximity to a junction, and they may provide critical safety information to the driver well in advance. A cooperative intelligent transportation system (C-ITS) has recently acquired popularity for its capacity to minimise red-light running, which improves road safety at junctions as well as pedestrian crossings. Here, connected vehicles communicate with each other and road infrastructure such as through cooperative awareness messages (CAMs) and produce safety warnings for road users' safety [38]. A detailed review of drivers' red-light running behaviour prediction and technologies for countermeasures is available in our recent research article (Komol et al. [10]).

3. Data Summary

In 2020–2021, the Queensland Department of Transport and Main Roads (TMR), in partnership with the iMOVE Cooperative Research Centre (iMOVE CRC) and Queensland University of Technology (QUT) undertook a C-ITS pilot study in the city of Ipswich, Australia, called ICVP. The field operation test aimed to investigate the potential safety benefit of C-ITS, where warning messages were available to improve drivers' awareness of advanced red-light warnings, turning on warnings for vulnerable road users, road hazard alerts, back-of-queue alerts, road works alerts, and in-vehicle speed information. These warnings are shown (i.e., triggered) to drivers through a human–machine interface (HMI) on the vehicle's front console. The second objective was to assess the users' perceptions and acceptance of the new technology.

The ICVP recruited 355 participants who had the equipment retrofitted in their vehicle for up to nine months. About 90 percent of participants were assigned to the "Treatment" group, where the HMI was activated to convey the safety warnings in visual and audio forms for six months and disabled for three months to collect their baseline driving data. The remaining ten percent of participants were placed in a control group for the entire nine-month period. The HMI did not show any warning messages to the control participants, but their driving data were still logged for comparison.

When a participant encountered a use case, two sorts of data were used to evaluate the driver's behaviour. Vehicle trajectory data, collected at 10 Hz, were logged within a CAM. This contained information such as speed, scenario ID, yaw rate, latitude, longitude, lateral and longitudinal acceleration, and the timestamp for each of these events. Drivers' movement trajectories in intersections were analysed and straight/turning movements at intersections were automatically labelled using a deep transfer learning technique which also helped in identifying and cleaning erroneous trajectories due to GPS error [39]. Data relevant to the encounter are the second category of data logged (referred to henceforth as a scenario). Signal Phasing and Timing (SPaT), at 10 Hz, from the intersection information was matched with CAMs for determining red-light running scenarios. This comprises timestamps for when the vehicle enters and departs a use case, identifying variables for the use case encountered, such as a junction or road work zone ID, if an HMI message is shown, and participant-related data like participant ID and whether HMI is enabled.

4. Methodological Framework

In order to model the red-light running and stopping behaviours of drivers at signalised intersections, vehicle kinematic information such as speed, speed limit, longitudinal acceleration, lateral acceleration, and yaw rate was monitored. Time-series RNN LSTM and GRU algorithms are used to examine the temporal change in vehicle kinematics when approaching intersections to predict driver red-light running behaviour in the C-ITS environment. A flowchart of red-light running behaviour prediction methodology is shown in Figure 2.

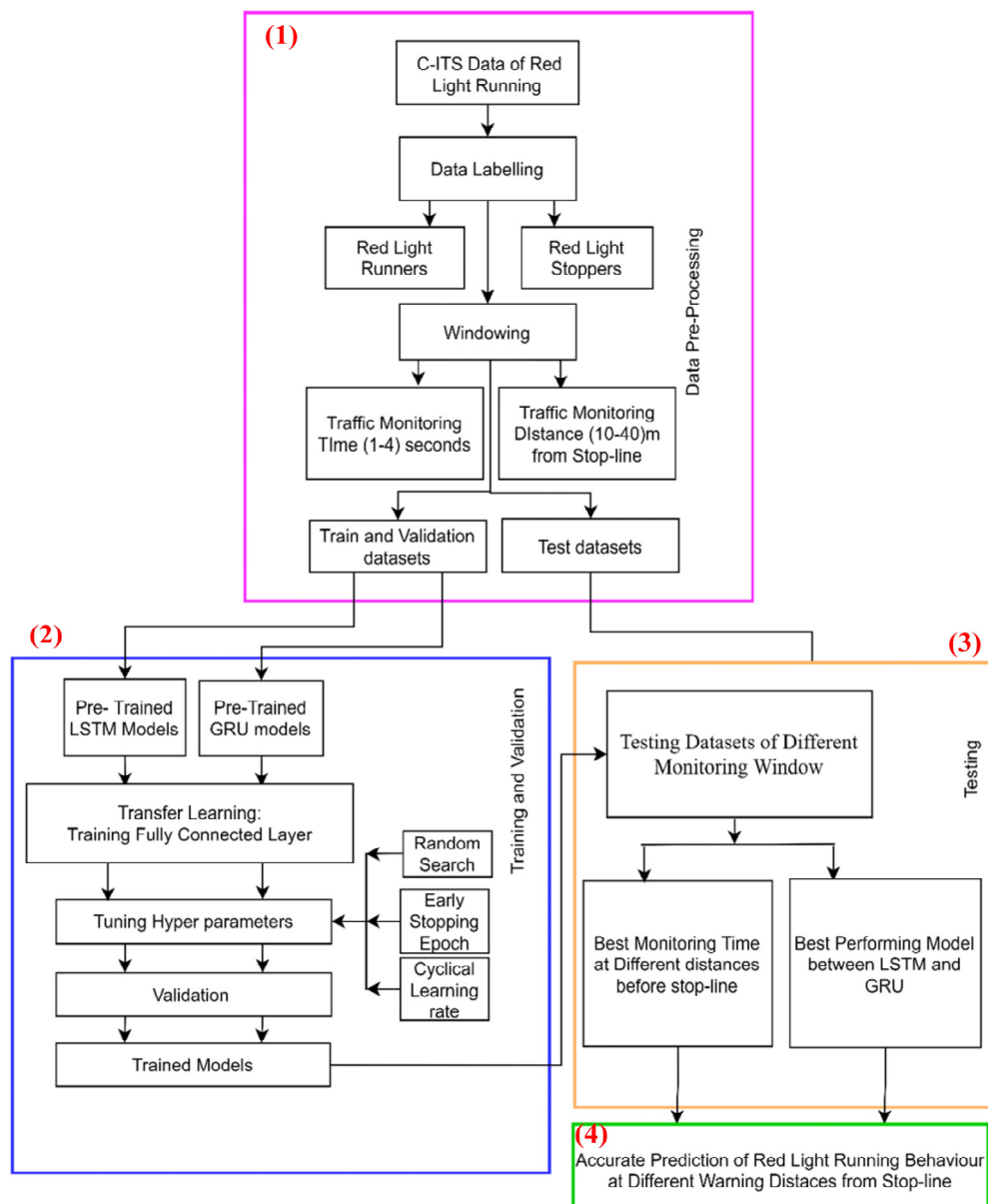


Figure 2. Flowchart of red-light running behaviour prediction methodology.

Due to the supervised learning nature of LSTM and GRU algorithms, the dataset must be labelled. The data-labelling process involved matching the vehicles' trajectory and SPaT data. Some decision rules were developed to screen the scenarios before examining the visualisation to confirm the outcome of each potential red-light running scenario. The scenario is given a label of 0 if someone did not run a red-light and 1 if they did. The dataset is then windowed from the FOT data for a duration ranging from 1 s to 4 s in different safety warning distances (10 m to 40 m) before the stop line (Figure 2: Box 1). Separate

prediction models were trained with different dataset windows to identify the optimal traffic monitoring time and evaluate the prediction accuracy at different early warning distances. However, after an initial stage of data labelling, a limited number of 40 red-light running incidents were found. To prepare a dataset of both red-light running and stopping scenarios, these 40 red-light running incidents were combined with 460 scenarios where the driver obeyed the signal and stopped at the red-light.

However, this limited dataset is still insufficient for training deep recurrent models. To remedy this, we use the transfer learning technique from the pre-trained LSTM and GRU models, previously trained using intersection movement data for different monitoring windows, and fine-tuned these by training fully connected (FC) and SoftMax layers with red-light running dataset whilst freezing the pre-trained layers [20] (Figure 2: Box 2). We tuned the model hyperparameters using the random search method (Figure 2: Box 2). We tested our models for different test datasets windowed based on different monitoring times and distances (Figure 2: Box 3), based on which we evaluated accurate prediction models for different traffic monitoring times at different warning distances before the stop line and compared the performance between the LSTM and GRU models (Figure 2: Box 4).

5. Data Preprocessing

The data source and feature information used for this model are discussed in the data summary (Section 3). For our analysis of drivers red-light running behaviour, it is necessary to filter incidents related to red-light activation within the C-ITS dataset. If a vehicle trajectory scenario did not contain a red light prior to, or while traversing an intersection, the scenario was considered irrelevant. Also, we have developed a supervised machine learning algorithm for the prediction of driver red-light running behaviour at the onset of the red-light. The filtered dataset requires accurate labelling between red-light running incidents and red-light stopping incidents. For any intersection trajectory, the scenario was considered red-light running when the approaching vehicle entered the conflict zone during the red signal phase. Vehicles obeying the red signal, and therefore stopped before the stop line, were considered red-light stoppers. Though initial filtering removed many irrelevant scenarios, some remained. The most common example of this is a vehicle that crosses the stop line and enters the conflict zone on a green or amber signal, followed by receiving a red signal. The false alarm issue was mostly caused by positioning inaccuracy or latency between the traffic light changing and the SPaT data being received by the vehicle. This did not constitute a red-light runner or stopper and these scenarios were discarded as well. This behaviour is illustrated in Figure 3a.

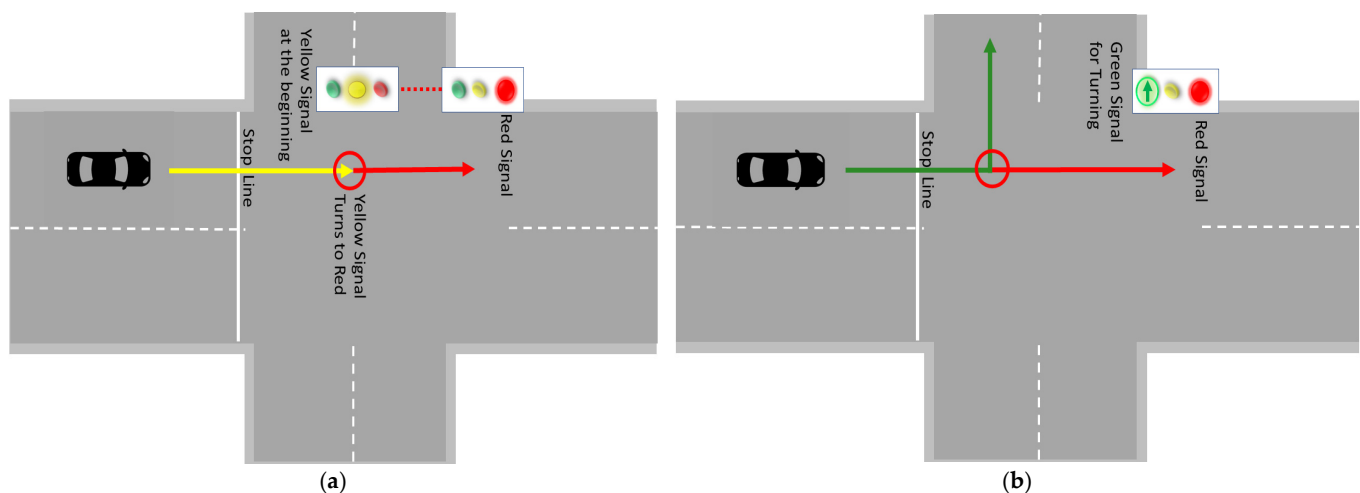


Figure 3. (a) Vehicle passing intersection during yellow signal which then turns red when the vehicle enters the conflict zone. (b) Vehicle turning during green signal but the straight signal is red [40].

Another scenario that was discarded for the purposes of analysis is shown in Figure 3b. Here, the vehicle intends to turn validly with a left-turn green; however, since the lane is shared with a straight through movement which is red, the vehicle algorithm is unable to determine on approach if the vehicle will go straight and therefore will warn the driver if the speed threshold is exceeded. In post-analysis, we were able to determine the vehicle-turning movement in such cases is legal and not considered a red-light violation.

Some incidents occurred where drivers initially stopped at the red signal, obeying the road rules, but became impatient and encroached on the stop bar before the red signal changed. These scenarios were also eliminated because the focus of this study is on early prediction and intervention of unsafe behaviour.

The data for Connected Intelligent Transportation Systems (C-ITSs) was gathered at a rate of 10 times per second and contained details such as vehicle speed, the recommended speed limit, how fast the vehicle was accelerating or decelerating, and how it was turning at various time points. This information was arranged in the order it occurred, starting from when the vehicle approached the intersection and stopped at the line. The abnormal trajectories and erroneous data caused by missing information or GPS errors were removed to eliminate noise from the dataset using our previous research methodology [39]. After filtering and labelling the data, around 40 valid red-light running incidents were found. Another 460 red-light stopping incidents were included to create a dataset of a total of 500 data samples which were used for training and testing models of driver red-light running behaviour prediction.

Another crucial factor to take into account in the prediction of intersection movements pertains to the timing of driver warnings through human-machine interaction (HMI). In addition to ensuring accurate predictions, it is essential to issue warnings as early as possible, allowing drivers ample time to respond and adjust their manoeuvres. However, it is important to note that as the warning distance from the intersection increases, the accuracy of predictions tends to decrease. To determine the optimal HMI warning distance, we divided the dataset into distinct sets, assessing various monitoring time intervals, ranging from 1 s to 4 s at different warning distances ranging from 10 m to 40 m before reaching the stop-line. Each individual dataset was then employed to train and test prediction models, enabling a comparison of prediction accuracy across different HMI warning distances and traffic monitoring durations. This analysis of prediction accuracy across varying monitoring distances and time intervals serves to find the suitable model for different HMI warning distances. Figure 4 shows the windowing of datasets with different traffic monitoring times at different distances before the stop line.

Here, the dataset was split to create separate datasets for different windows, with each then being split into a train-validation-test ratio of 70-10-20%. Training-validation datasets of different windows were then input into RNN models separately to train individual prediction models for different warning distances. The models were then tested with a test dataset to identify the best traffic monitoring time and the accuracy of the prediction models at different distances before the stop line.

Our study thoroughly assessed how well different time periods and distances from the stop line could predict driving conduct. In order to provide a thorough perspective of how drivers interact with red-light signals, a 4 s, 40 m scenario was used for the assessment. However, it was also investigated how different distances and shorter and longer time periods affected the accuracy and relevance of the forecasts. Shorter time periods, like one or two seconds, are beneficial for situations that call for quick system actions, according to our findings. Longer windows of up to 4 s, on the other hand, improve the ability to take preventative action by giving the system and the driver enough time to respond suitably.

The time window must be chosen carefully and in accordance with the particular operational goals of the traffic management system in use. The human-machine interface (HMI) can trigger warnings adaptively based on the current needs necessitated by varied traffic situations because the time period chosen is flexible enough to accommodate varying traffic dynamics. In order to guarantee precise behavioural forecasts and safe decision-

making, longer monitoring durations may be required for the behaviour of longer vehicles, which may decelerate more gradually due to their size. A shorter monitoring period may be adequate for quick decisions involving fast-moving vehicles in high-traffic situations during peak hours, while unfavourable weather conditions like rain may necessitate longer observation times to account for reduced vehicle handling and visibility. This careful method guarantees that the predictive system will continue to be accurate and adaptable, meeting the various needs brought forth by different traffic situations and vehicle types.

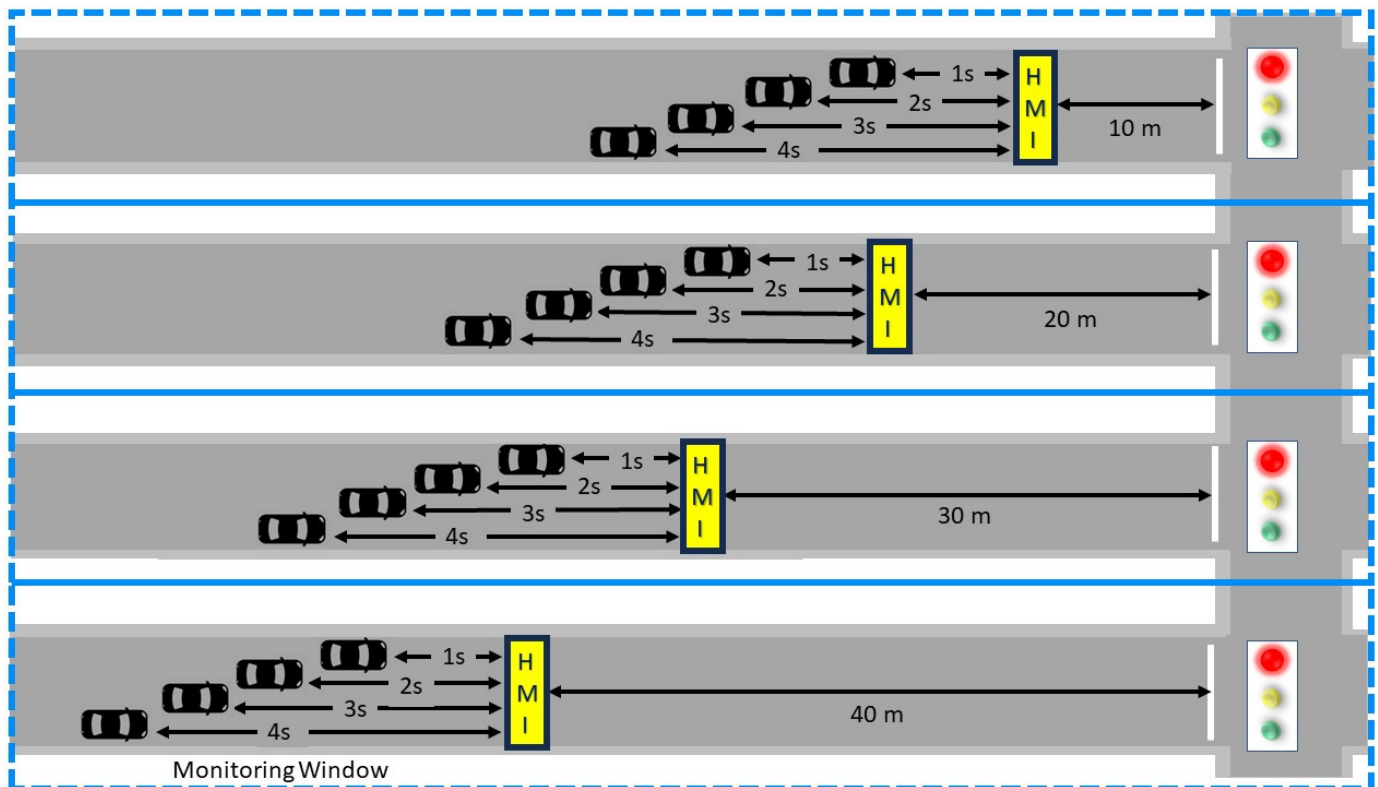


Figure 4. The windowing of datasets with different traffic monitoring times at different distances before the stop line [20].

6. Model Justification and Hyperparameter Tuning

In the hypothesis from Section 1, deep RNNs such as LSTM and GRU are considered good for the purposes of predicting driver red-light running and stopping behaviour, which is exhibited as a change in approaching vehicle' kinematics. For example, the speeding behaviour of red-light stoppers is expected to reduce gradually before the stop line, whereas red-light runners hardly show a speed reduction or accelerate to run the intersection. So, RNN models are suitable for this study with the LSTM and GRU being considered good deep learning models in terms of overcoming the gradient vanishing problems of neural network and outperforming traditional recurrent networks. These models eventually outperform each other in different applications, and hence, we consider them both to identify the best model for this study. Since this dataset has only 500 samples, we used fine-tuning and transfer learning with pre-trained LSTM and GRU models, previously trained in intersection movement prediction [20]. The existing layers of GRU and LSTM models are kept frozen, and the FC layer is trained with a red-light running dataset of 375 samples (30 red-light running and 345 red-light stopping). We tuned the hyperparameters with a random search hyperparameter optimisation method using the Optuna Python library [41]. The hyperparameter values were set in a grid range of values, and the models were trained with different values within the range. The input values for turning hyper-parameters of our models are shown in Table 1.

Table 1. Random grid of hyperparameter values.

Hyper-Parameter	Value Range	Search Type
Batch Size	15 to 200	Integer range
Optimiser	Adam, SGD, RMSprop	String categorical
Learning Rate	0. 1 to 0.00001	Float range
Epoch Number	4 to 35	Integer range

We employed a cyclical learning rate approach to dynamically adjust our learning rate, exploring a range of values within reasonable boundaries for this parameter [42]. Consequently, both random search and cyclical methods were employed to fine-tune the learning rate, aiming to identify the optimal learning rate that minimises the loss function gradient during model training. To determine the number of training epochs, we implemented an early stopping criterion [43], which required a minimum of 15 epochs without an improvement in validation accuracy. In such cases, training ceased, and the epoch with the highest validation accuracy among the last 15 epochs was deemed the optimal epoch number. This approach not only expedited the random search process but also facilitated more precise tuning of the epoch number by preventing the selection of excessive epoch values, which could lead to overfitting or underfitting issues. Overfitting occurs when too many epochs cause the model to fit the training data excessively, surpassing the global optimum of the loss function gradient. Conversely, underfitting results from an insufficient number of epochs, causing the model to fail to reach the global optimum. Both overfitting and underfitting hinder the accurate optimisation of the model, thereby impairing its performance on test data.

We conducted a total of 100 random search trials, with each model having a maximum training time of 3.5 h. Upon completion of these trials, the model with the highest validation accuracy was selected, along with its corresponding hyperparameters. These hyperparameters were further fine-tuned to train the models for the classification of driver red-light running behaviour.

To assess prediction accuracy at various warning distances (10 m, 20 m, 30 m, and 40 m before the stop line) and determine the optimal traffic monitoring time, we trained separate models using windowed data for different distances.

7. Model Architecture

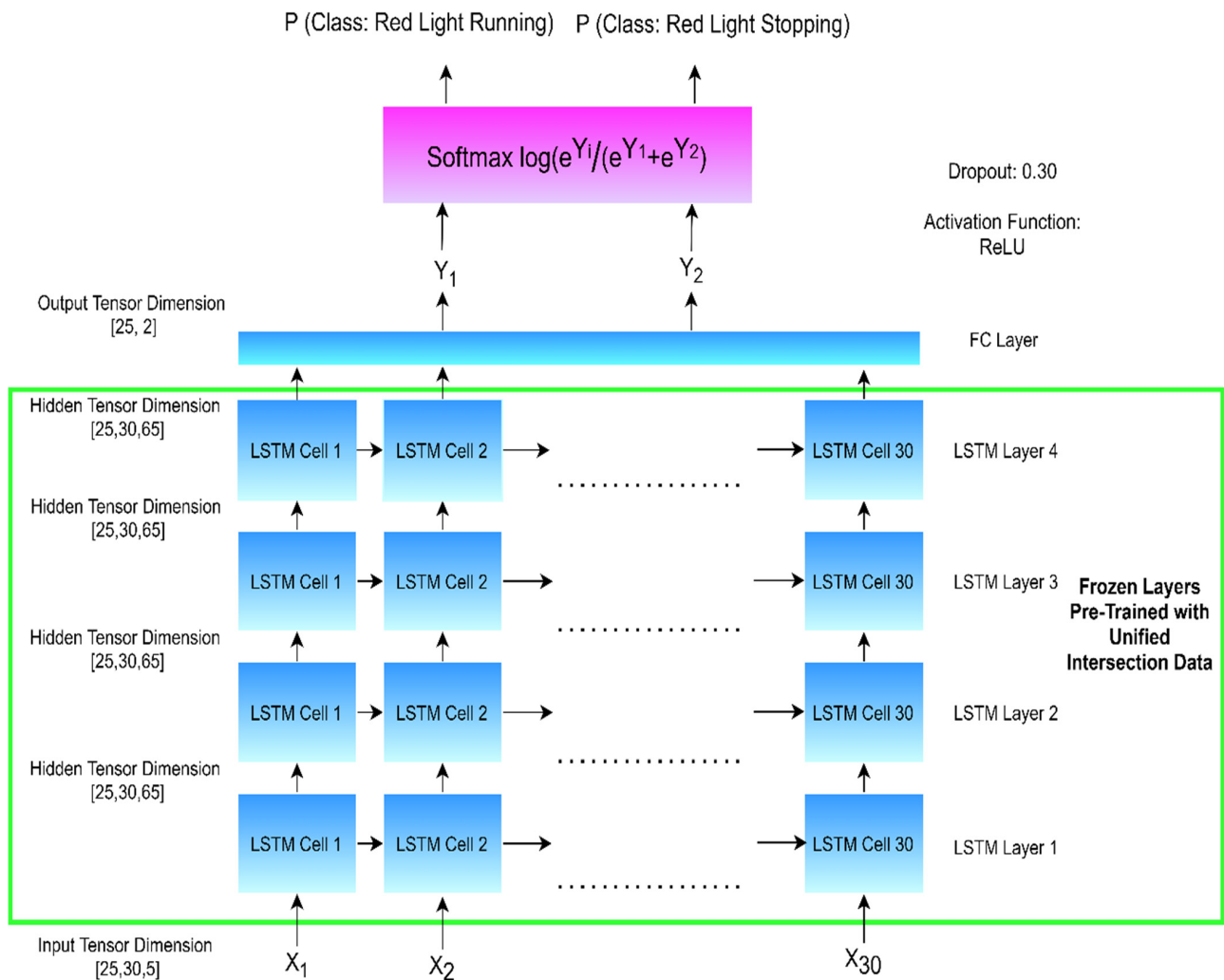
Figure 5 shows the model architecture after training with the pre-trained LSTM model for 3 s traffic monitoring at 10 m distances from the stop line.

In this context, we take a pre-trained LSTM model that was originally trained using combined intersection data to predict vehicle turning movements [20]. We then refine this model by training it specifically on red-light running data. To enhance the model's ability to predict turning movements, we conduct separate training sessions for both LSTM and GRU models. During this training, we increase the representation of turning movement samples through data upsampling, but this upsampling is exclusively applied to the training dataset. This distinction is made to prevent any bias when assessing the model's performance in predicting both straight and turning movements.

In this study, we employ pre-trained LSTM models, data-augmented pre-trained LSTM models, pre-trained GRU models, and data-augmented pre-trained GRU models, employing a transfer learning approach. The LSTM and GRU layers of the pre-trained model are kept fixed, while only the fully connected (FC) layer is trained using red-light running data. Fine-tuning is limited to determining the batch size, learning rate, optimiser choice, and identifying the optimal number of epochs.

Since the data were gathered at a 100-millisecond interval, every second comprises 10 data points. To accommodate a 3 s monitoring window, we use a sequence dimension of 30 data points. We set the batch size to 25, with an input size of 5 features, resulting in an input dimension of [5,25,30]. The sequence dimension and neuron count of the hidden layers remain constant as they belong to the frozen layers of the pre-trained model. The

outputs (Y_1 and Y_2) from the fully connected layer are subjected to the logarithm of the SoftMax function to estimate the probabilities associated with the red-light running and stopping classes.



Input, X = Input Features (Speed, Speed limit, Longitudinal Acceleration, Lateral Acceleration, Yaw rate)

Dataset: Red Light Running and Stopping Data

Figure 5. Transfer learning with pre-trained LSTM model to predict red-light running behaviour.

8. Results and Discussion

After training separate prediction models for different traffic monitoring times of 1 s, 2 s, 3 s, 4 s at different warning distances of 10 m, 20 m, 30 m, 40 m before the stop-line, each model was then tested with the remaining 20% of data (125 data samples: 10 red-light running and 115 red-light stopping), and model performance was evaluated at different distances. The optimal periods for traffic monitoring were found to be 1 s and 3 s. These intervals yield the highest accuracy in predicting red-light violations at various warning distances before the stop line. The comparison of red-light running and stopping prediction accuracy using pre-trained LSTM and GRU models of before and after data upsampling is shown in Tables 2 and 3.

Table 2. Results of LSTM model on red-light running behaviour prediction.

Distance from Stop-Line	Accuracy (%)	Pre-Trained LSTM				Data Upsampled Pre-Trained LSTM			
		1 s	2 s	3 s	4 s	1 s	2 s	3 s	4 s
10 m	Overall	71.3	63.1	72.7	68.6	72.9	64.7	60.3	52.0
	RLS	72.3	62.5	72.9	67.5	74.1	63.3	65.7	49.5
	RLR	70	70	70	80	60	80	70	80
20 m	Overall	72.7	71.0	72.7	65.2	70.2	66.1	60.3	56.7
	RLS	72.0	71.1	73.8	64.8	70.2	64.8	58.5	55.5
	RLR	80	70	60	70	70	80	80	70
30 m	Overall	67.7	54.5	69.7	53.3	73.5	67.7	51.2	59.3
	RLS	67.5	53.1	70.6	51.8	73.8	67.5	48.6	57.4
	RLR	70	70	60	70	70	70	80	80
40 m	Overall	70.9	60.6	58.6	62.4	69.2	64	65.5	51
	RLS	71.9	59.8	58.4	63	70	63	66	55
	RLR	60	70	60	50	60	70	50	70

Table 3. Results of GRU model on red-light running behaviour prediction.

Distance from Stop-Line	Accuracy (%)	Pre-Trained GRU				Data Upsampled Pre-Trained GRU			
		1 s	2 s	3 s	4 s	1 s	2 s	3 s	4 s
10 m	Overall	65.5	50.8	60.3	42.1	65.5	51.6	59.5	65.2
	RLS	65.1	47.3	58.5	37.8	65.1	48.2	58.5	64.8
	RLR	70	90	80	90	70	90	70	70
20 m	Overall	69.4	68.6	66.9	78.8	71.9	50.4	64.4	86.4
	RLS	69.3	68.4	66.6	79.6	71.1	46.8	63.9	88.8
	RLR	70	70	70	70	80	90	70	60
30 m	Overall	68.6	70.2	68.9	58.4	69.4	56	74.7	61
	RLS	67.5	69.3	69.7	58.2	69.3	54	76.1	60
	RLR	80	80	60	60	80	80	60	70
40 m	Overall	69.2	66.6	64.6	50.4	64.1	62.4	56	54
	RLS	70	66.3	65	50.4	63	62.6	53	57
	RLR	60	70	60	50	70	60	80	70

Analysing Tables 2 and 3, the LSTM model shows better accuracy than the GRU model when predicting drivers' red-light running and red-light stopping behaviours at intersections. The data upsampled pre-trained LSTM model shows the highest overall prediction accuracy (73.55%) for 1 s traffic monitoring at a 30 m distance before the stop. The overall prediction accuracy by the data upsampled pre-trained LSTM model slightly varies for 1 s traffic monitoring at different warning distances but stays around 70% on average. The pre-trained LSTM model without upsampled data shows nearly similar prediction accuracy for 1 s and 3 s traffic monitoring but its accuracy drops significantly at 30 m and 40 m warning distances, respectively. The average overall prediction accuracy using GRU models is below 70%. So, the data upsampled pre-trained LSTM model is considered befitting for overall red-light running and red-light stopping behaviour prediction for 1 s traffic monitoring at different warning distances. For individual red-light stopping behaviour prediction, both the data upsampled pre-trained LSTM model and the regular pre-trained LSTM model without upsampled data show the highest accuracy for 1 s traffic monitoring at different warning distances. However, the regular pre-trained LSTM model without upsampled data shows better prediction accuracy for individual red-light running behaviour prediction than the data upsampled pre-trained LSTM model.

For pre-trained LSTM models, data upsampled pre-trained LSTM models, pre-trained GRU models and data upsampled pre-trained GRU models, the comparison of red-light running and red-light stopping behaviour prediction accuracy is shown in Figure 6.

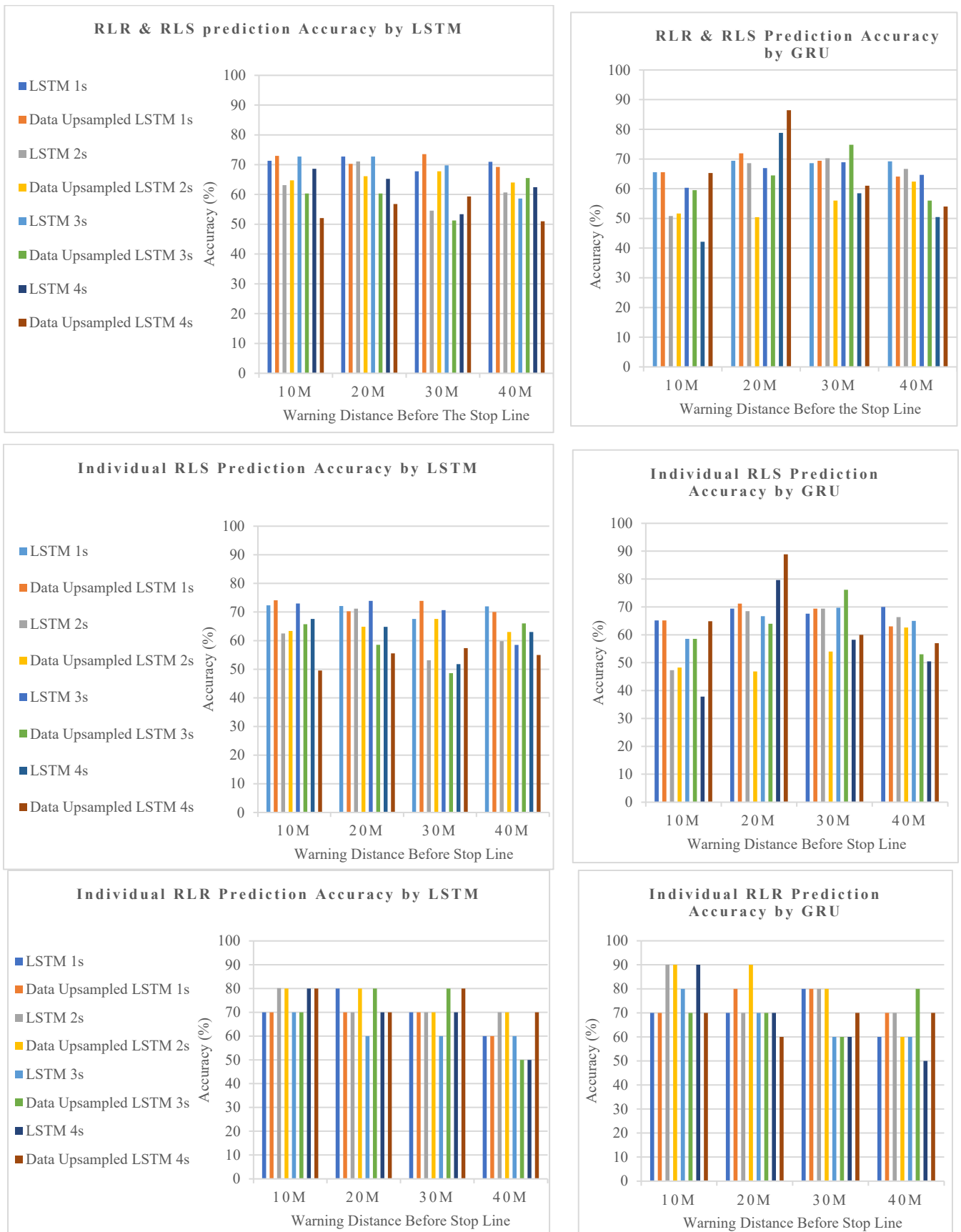


Figure 6. The comparison of LSTM and GRU models’ prediction accuracy before and after data upsampling.

In this comparative analysis of traffic red-light running prediction accuracy, we investigate the efficacy of regular and data upsampled models employing Long Short-Term Memory (LSTM) and Gated Recurrent Unit (GRU) networks across varying warning distances. It is observed that regular prediction models utilising both LSTM and GRU architectures exhibit superior accuracy compared to their upsampled counterparts. Specifically, in predicting individual red-light stopping incidents, the regular LSTM and GRU models consistently outperform the data upsampled models at various distances. However, an exception is noted at a 30 m, 4 s window, where the upsampled LSTM model demonstrates marginally higher accuracy in predicting red-light stopping events than the regular LSTM model.

Moreover, the regular LSTM and GRU models show enhanced performance in accurately predicting red-light stopping events compared to data upsampled models at different warning distances. The accuracy of both LSTM and GRU models with the upsampled dataset significantly improves predictions of individual red-light running samples, achieving a uniform balance with red-light stopping predictions. Overall, the regular LSTM model maintains more consistent accuracy in predicting red-light running and stopping behaviours, surpassing both the upsampled models and GRU models. Conversely, while the GRU model exhibits comparable levels of accuracy, its performance is not as consistent as that of the LSTM model, peaking at nearly 90% during a 4 s traffic monitoring interval at a 20 m distance before the stop line.

Crucially, the faster prediction capabilities of the GRU model afford drivers additional time to assess and make informed decisions. Given the GRU algorithm's simplicity, coupled with its lower memory and computational demands, it holds significant potential for integration into Intelligent Transportation Systems (ITSs).

In short, the plots show the prediction accuracy of transfer learning models using GRU and LSTM models pre-trained with intersection red-light running and stopping data input. Analysing the performance of pre-trained LSTM and GRU models to predict red-light running behaviour, the performance of the regular LSTM model pre-trained was found to be the most resilient and robust in predicting overall red-light running and stopping behaviour for 1 s traffic monitoring, which is around 72.95%, 70.25%, 73.55% and 69.23% at 10 m, 20 m, 30 m and 40 m before the stop line.

Given the dataset's imbalanced nature, it is premature to make a recommendation favouring the LSTM model trained with upsampled data over the regular GRU model without first conducting a comprehensive assessment using various performance metrics. These metrics encompass sensitivity, specificity, precision, negative predictive value (NPV), and the F1 score.

Sensitivity and specificity, also referred to as true positive rates and true negative rates, respectively, play a crucial role in our binary classification scenario, where we aim to predict red-light running and red-light stopping behaviours. Sensitivity measures the accurate identification of red-light stopping instances relative to the total number of samples predicted as red-light stopping, which includes red-light running samples erroneously categorised as red-light stopping. Conversely, specificity quantifies the precise identification of red-light running instances compared to the total number of samples predicted as red-light running, encompassing red-light stopping samples incorrectly classified as red-light running. Precision denotes the accurate prediction of red-light stopping instances concerning the total number of existing red-light stopping samples. Negative predictive value assesses the accurate prediction of red-light running instances in relation to the total number of existing red-light running samples. The F1 score, calculated as the harmonic mean of precision and sensitivity, provides a comprehensive performance measure.

We applied these performance metrics to evaluate the prediction of red-light stopping and running behaviour using the pre-trained LSTM model, the upsampled data pre-trained LSTM model, the pre-trained GRU model, and the upsampled data pre-trained GRU model. These models underwent training and testing using data gathered from all 29 intersections.

The performance matrix analysis for different models predicting intersection movements with 3 s traffic monitoring at various warning distances is presented in Table 4.

Table 4. Performance measurements of LSTM and GRU models on RLR behaviour prediction.

Distance Before the Stop Line	Measurements	Pre-Trained LSTM	Data Upsampled Pre-Trained LSTM	Pre-Trained GRU	Data Upsampled Pre-Trained GRU
10 m	Sensitivity	95.29%	95.40%	96.05%	96.05%
	Specificity	16.22%	17.14%	15.22%	15.22%
	Precision	72.32%	74.11%	65.18%	65.18%
	NPV	60.00%	60.00%	70.00%	70.00%
	F1 Score	82.23%	83.42%	77.66%	77.66%
20 m	Sensitivity	97.56%	96.30%	96.25%	98.11%
	Specificity	20.51%	17.50%	17.07%	13.24%
	Precision	72.07%	70.27%	69.37%	46.85%
	NPV	80.00%	70.00%	70.00%	90.00%
	F1 Score	82.90%	81.25%	80.63%	63.41%
30 m	Sensitivity	96.15%	96.47%	97.40%	95.40%
	Specificity	16.28%	19.44%	18.18%	18.75%
	Precision	67.57%	73.87%	67.57%	76.15%
	NPV	70.00%	70.00%	80.00%	60.00%
	F1 Score	79.37%	83.67%	79.79%	84.69%
40 m	Sensitivity	93.94%	95.77%	94.94%	95.77%
	Specificity	12.00%	15.22%	15.79%	15.22%
	Precision	58.49%	63.55%	70.09%	63.55%
	NPV	60.00%	70.00%	60.00%	70.00%
	F1 Score	72.09%	76.40%	80.65%	76.40%

From Table 4, the LSTM models show better performance than the GRU models considering that the GRU models' precision (accurate prediction of red-light stopping behaviour) highly reduces the models' performance at different traffic warning distances. The pre-trained LSTM models show slightly different performance than data-upsampled pre-trained LSTM models, which outperform the pre-trained LSTM models at 10 m, 30 m, and 40 m before the stop line. Only at 20 m before the stop line does the pre-trained LSTM model show slightly higher performance than the data-upsampled pre-trained LSTM model analysing all performance measure matrices. A bar chart of the LSTM and GRU models' performance measure matrices' comparison is shown in Figure 7.

High negative predictive value (NPV) is a desired outcome for models that classify red-light violation as NPV measures the true predicted red-light running samples out of actual existing red-light running samples. The NPV score significantly increases for GRU models at a warning distance of 10 m before the stop line, providing clear evidence of improved red-light running prediction performance by GRU models. The data upsampled pre-trained GRU model achieves a 90% NPV score at a 20 m distance from the stop line, while the regular pre-trained GRU model achieves a 70% NPV score in this aspect. Similarly, high NPV scores for predicting red-light running samples can be observed for GRU models at distances of 30 m and 40 m before the stop line. Given the importance of selecting a model that focuses on predicting red signal violations, GRU models, especially the data upsampled pre-trained GRU models, are highly recommended. However, GRU models are less balanced when it comes to predicting both red-light running and red-light stopping behaviour samples. In contrast, LSTM models demonstrate good performance in predicting red-light running samples (with a good NPV score) while also maintaining a balanced performance in predicting red-light stopping behaviour samples, as evidenced by sensitivity, specificity, and precision score analysis. By examining the bar graph in Figure 7, it becomes evident that the sensitivity value exceeds the specificity value at various warning distances. This indicates that the proportion of accurately predicted red-light stopping behaviour samples to the total number of samples predicted as red-light stopping is relatively higher than the proportion of accurately predicted red-light running samples to

the total number of samples predicted as red-light running. Furthermore, the sample size of red-light stopping behaviour is larger than that of red-light running, which contributes to the decrease in specificity values for GRU models at different warning distances. The F1 score also decreases when using GRU models as the number of accurately predicted red-light running samples decreases. In summary, pre-trained GRU models are highly effective in predicting red-light running behaviour compared to regular pre-trained GRU models and LSTM models, but they do not ensure a balanced prediction of both classes: red-light running and red-light stopping behaviour. However, for specific applications where the prediction of red-light running is the primary focus, the pre-trained GRU model may be more effective. Overall, the pre-trained LSTM model is highly recommended for achieving a balanced performance in predicting both red-light running and red-light stopping behaviour classes.

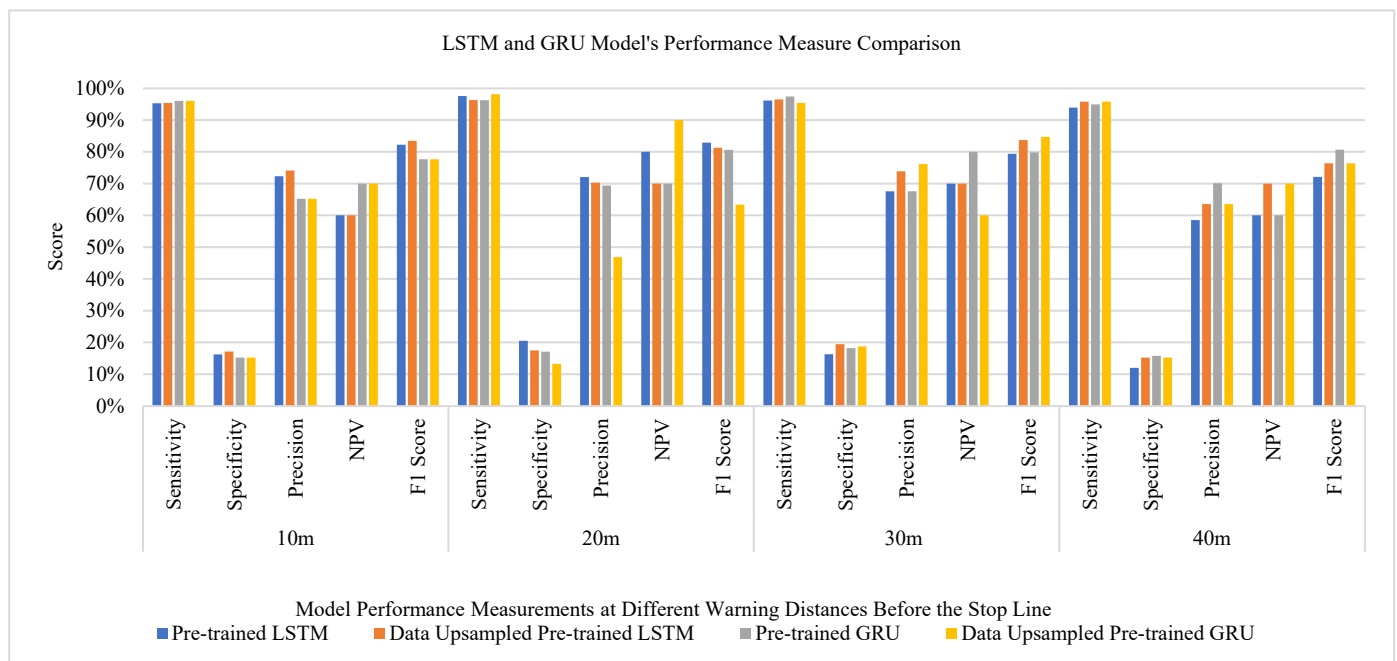


Figure 7. The comparison of LSTM and GRU models' performance measures.

In a practical context, 100% accuracy with prediction and on-road variables is not possible. Implementation of this should initially be as a complimentary support alert where the driver is in control and responsible. Optimising the driver warnings to suit the likelihood and impact of true positive and false positive situations should be considered to minimise any adverse impacts (e.g., distraction, annoyance).

9. Conclusions

This research paper presents a groundbreaking study conducted within the framework of the ICVP project in Queensland, Australia. The primary focus of this investigation was to predict red-light running behaviour in signalised intersections within a connected vehicle environment, employing recurrent neural networks, specifically LSTM (Long Short-Term Memory) and GRU (Gated Recurrent Unit) architectures. This research introduced LSTM and GRU models for the first time in the context of the largest field operation test conducted in Australia. These neural network architectures were employed to analyse and forecast driver behaviour at signalised intersections, providing novel insights into red-light running tendencies, which helps in the accurate prediction of red-light running behaviour. To address the challenge posed by the limited dataset, a transfer learning approach was strategically employed. This method leveraged knowledge and pre-trained models from prior research focused on predicting drivers' intended movements at intersec-

tions. This innovative application of transfer learning effectively mitigated the constraints imposed by the scarcity of red-light running scenarios within the dataset, establishing a robust foundation for predictive analysis. A significant contribution of this study lies in its ability to transfer the learning of model from our previous research on drivers' intended movement prediction [20] to create a new model to predict red-light violations at various warning distances before the stop line. This predictive capability holds immense potential for enhancing traffic safety through the timely deployment of precautionary measures, such as connected vehicle warnings, precise signal timing management, and adaptive all-red signal extensions. Furthermore, this research identified and developed models that strike a delicate balance between predicting red-light running and stopping behaviours while simultaneously prioritising the accurate prediction of red-light violations as a stringent constraint.

The analysis of predictive models for red-light running and red-light stopping behaviours reveals that the highest prediction accuracy was achieved with 3 s and 1 s traffic monitoring intervals. Notably, the proportion of accurately predicted instances of vehicles stopping at red lights is significantly higher compared to the proportion of accurately predicted red-light running cases. The performance evaluation of LSTM and GRU models demonstrates the superior effectiveness of pre-trained GRU models in red-light running prediction when contrasted with conventional pre-trained GRU models and LSTM models. Nevertheless, it is noteworthy that GRU models exhibit an imbalance in predicting both red-light running and red-light stopping behaviours. However, for specialised applications emphasising red-light running prediction, the pre-trained GRU model may offer heightened efficacy. In a broader context, the pre-trained LSTM model is strongly recommended to attain a balanced predictive performance encompassing both red-light running and red-light stopping behaviours categories. These distinctions highlight the importance of model selection based on specific traffic management goals. Implementing these predictive models as supplementary driver alerts can enhance road safety by mitigating potential distractions and optimising driver response strategies. Overall, the choice between GRU and LSTM models should be guided by the specific needs of traffic monitoring and management systems, aiming to maximise safety and efficiency on the roads.

This research benefits in safeguarding against hazardous situations like right angle collisions and head-on collisions, thereby reinforcing traffic safety. Additionally, this work extends its implications to vulnerable road users, including pedestrians and cyclists, by facilitating the provision of safety warnings when they traverse intersections. Moreover, early detection of red-light violations can prompt distracted or impaired drivers, whether due to drugs or alcohol, to respond to a warning and avoid committing a traffic offence or being involved in an accident.

In short, this research represents a significant advancement in the domain of traffic safety and management within a connected vehicle environment. By introducing LSTM and GRU models and leveraging transfer learning techniques to tackle the limited dataset issue, this study not only contributes to the early detection of red-light running behaviour but also establishes a comprehensive framework for enhancing road safety and efficiency for both motorists and vulnerable road users.

A more thorough examination of the effects of varied deceleration behaviours across various time periods on red-light breaches will be possible with future research that integrates interpretable and explainable AI models. For instance, one car might start to slow down four seconds earlier, while another might abruptly slow down two seconds earlier. Through a thorough case study, future research might also examine how these predictive insights might be incorporated into policy applications. In addition to showcasing the forecasts' usefulness, this would highlight how they could be applied to improve road safety and traffic light cycles. These kinds of studies would offer verifiable illustrations of how predictive models might impact and enhance traffic control systems.

Author Contributions: Conceptualisation, M.M.R.K. and M.E.; methodology, M.M.R.K.; software, M.M.R.K. and J.P.; validation, M.M.R.K. and M.E. formal analysis, M.M.R.K. and M.E.; investigation, M.M.R.K., M.E., S.G., M.W. and D.A.; resources, M.M.R.K., M.E. and A.R.; data curation, M.M.R.K., M.E. and J.P.; writing—original draft preparation, M.M.R.K.; writing—review and editing, M.M.R.K., M.E., J.P., M.M., S.G., M.W. and D.A.; visualisation, M.M.R.K., M.E., J.P., M.M., S.G., M.W. and D.A.; supervision, M.E., M.M. and A.R.; project administration, M.E., M.M. and A.R.; funding acquisition, M.E., M.M. and A.R. All authors have read and agreed to the published version of the manuscript.

Funding: This research received no external funding.

Data Availability Statement: This dataset is confidential for public access. This dataset is taken from the Queensland Department of Transport and Main Roads, Australia.

Acknowledgments: Profound acknowledgement goes to the Department of Transport and Main Roads (Queensland), Australia, for providing the data of our current study. The data were collected for ICVP, which was delivered by the Department of Transport and Main Roads, supported by the Motor Accident Insurance Commission, QUT's Centre for Accident Research and Road Safety—Queensland, iMOVE Australia, Telstra, Ipswich City Council and the Department of Infrastructure, Transport, Regional Development and Communications.

Conflicts of Interest: The authors declare no conflicts of interest.

References

1. World Health Organisation. *Global Status Report on Road Safety 2018*; World Health Organisation: Geneva, Switzerland, 2018.
2. International Transport Forum. *Road Safety Annual Report*; OECD Publishing: Paris, France, 2018. [CrossRef]
3. Shahariar, G.M.H.; Bodisco, T.A.; Surawski, N.; Komol, M.R.; Sajjad, M.; Chu-Van, T.; Ristovski, Z.; Brown, R.J. Real-driving CO₂, NO_x and fuel consumption estimation using machine learning approaches. *Next Energy* **2023**, *1*, 100060. [CrossRef]
4. Komol, M.R.; Hasan, M.; Elhenawy, M.; Yasmin, S.; Masoud, M.; Rakotonirainy, A. Crash severity analysis of vulnerable road users using machine learning. *PLoS ONE* **2021**, *16*, e0255828. [CrossRef] [PubMed]
5. Porter, B.E.; England, K.J. Predicting Red-Light Running Behavior: A Traffic Safety Study in Three Urban Settings. *J. Saf. Res.* **2000**, *31*, 1–8. [CrossRef]
6. IIHS. *Red Light Running*; Insurance Institute for Highway Safety (IIHS): Arlington, TX, USA, 2023; Available online: <https://www.iihs.org/topics/red-light-running> (accessed on 14 May 2023).
7. Zhang, Y.; Yan, X.; Li, X.; Wu, J.; Dixit, V.V.; Zhang, Y.; Yan, X.; Li, X.; Wu, J.; Dixit, V.V. Red-Light-Running Crashes' Classification, Comparison, and Risk Analysis Based on General Estimates System (GES) Crash Database. *Int. J. Environ. Res. Public Health* **2018**, *15*, 1290. [CrossRef] [PubMed]
8. Qian, H.-B.; Dong, Y.-P. Engineering Countermeasures to Reducing Red-Light Running. In Proceedings of the 2009 IITA International Conference on Control, Automation and Systems Engineering (CASE 2009), Zhangjiajie, China, 11–12 July 2009; pp. 342–344.
9. Beck, D.; Tripathi, S. *Investigation of Key Crash Types: Rear-end Crashes in Urban and Rural Environments*; Austroads Research Report; Austroads Ltd.: Sydney, Australia, 2015.
10. Komol, M.R.; Pinnow, J.; Elhenawy, M.; Yasmin, S.; Masoud, M.; Glaser, S.; Rakotonirainy, A. A Review on Drivers' Red Light Running Behavior Predictions and Technology Based Countermeasures. *IEEE Access* **2022**, *10*, 25309–25326. [CrossRef]
11. Fuller, R.; Bates, H.; Gormley, M.; Hannigan, B.; Stradling, S.; Broughton, P.; Kinneer, N.; O'dolan, C. The conditions for inappropriate high speed: A review of the research literature from 1995 to 2006. *Transport* **2008**, 1–96. Available online: <http://worldcat.org/isbn/9781906581329> (accessed on 14 May 2023).
12. Pawar, N.M.; Khanuja, R.K.; Choudhary, P.; Velaga, N.R. Modelling braking behaviour and accident probability of drivers under increasing time pressure conditions. *Accid. Anal. Prev.* **2020**, *136*, 105401. [CrossRef]
13. Velez, E.R.; Horvath, I.; Vegte, W.v.d. A pilot study to investigate time pressure as a surrogate of being in haste. In Proceedings of the Ninth International Symposium on Tools and Methods of Competitive Engineering—TCME-2012, Karlsruhe, Germany, 7–11 May 2012; pp. 393–406.
14. Li, M.; Chen, X.; Lin, X.; Xu, D.; Wang, Y. Connected vehicle-based red-light running prediction for adaptive signalized intersections. *J. Intell. Transp. Syst.* **2016**, *22*, 229–243. [CrossRef]
15. Wang, L.; Zhang, L.; Zhang, W.-B.; Zhou, K. Red light running prediction for dynamic all-red extension at signalized intersection. In Proceedings of the 2009 12th International IEEE Conference on Intelligent Transportation Systems (ITSC), St. Louis, MO, USA, 4–7 October 2009; pp. 1–5.
16. Wang, L.; Zhang, L.; Zhou, K.; Zhang, W.-B.; Wang, X. Prediction of Red-Light Running on Basis of Inductive-Loop Detectors for Dynamic All-Red Extension. *Transp. Res. Rec. J. Transp. Res. Board* **2012**, *2311*, 44–50. [CrossRef]
17. Zhang, L.; Zhou, K.; Zhang, W.-B.; Misener, J.A. Prediction of Red Light Running Based on Statistics of Discrete Point Sensors. *Transp. Res. Rec. J. Transp. Res. Board* **2009**, *2128*, 132–142. [CrossRef]

18. Li, P.; Li, Y.; Guo, X. A Red-Light Running Prevention System Based on Artificial Neural Network and Vehicle Trajectory Data. *Comput. Intell. Neurosci.* **2014**, *2014*, 892132. [[CrossRef](#)] [[PubMed](#)]
19. Bailey, M. Road Safety Week Gives the Green Light for Hold the Red. Queensland Government Media State Website. Available online: <https://statements.qld.gov.au/statements/97730> (accessed on 14 May 2023).
20. Komol, M.R.; Elhenawy, M.; Masoud, M.; Rakotonirainy, A.; Glaser, S.; Wood, M.; Alderson, D. Deep RNN Based Prediction of Driver's Intended Movements at Intersection Using Cooperative Awareness Messages. *IEEE Trans. Intell. Transp. Syst.* **2023**, *24*, 6902–6921. [[CrossRef](#)]
21. TMR. Ipswich Connected Vehicle Pilot Safety Evaluation. Department of Transport and Main Roads, Queensland. iMOVE Australia Website, Queensland. May 2022. Available online: <https://imoveaustralia.com/wp-content/uploads/2022/06/IVCP-Safety-Evaluation.pdf> (accessed on 14 May 2023).
22. Pugh, N.; Park, H. Prediction of Red-Light Running using an Artificial Neural Network. In Proceedings of the SoutheastCon 2018, St. Petersburg, FL, USA, 19–22 April 2018; pp. 1–4.
23. Zahid, M.; Jamal, A.; Chen, Y.; Ahmed, T.; Ijaz, M. Predicting Red Light Running Violation Using Machine Learning Classifiers. In *Green Connected Automated Transportation and Safety*; Wang, W., Chen, Y., He, Z., Jiang, X., Eds.; Springer: Singapore, 2022; pp. 137–148.
24. Shen, W.; Zhang, X.; Wang, X.; Feng, J. Violation target detection based on video streaming. In Proceedings of the 2020 International Conference on Computer Engineering and Intelligent Control (ICCEIC), Chongqing, China, 6–8 November 2020; pp. 203–206.
25. Chen, X.; Zhou, L.; Li, L. Bayesian network for red-light-running prediction at signalized intersections. *J. Intell. Transp. Syst.* **2019**, *23*, 120–132. [[CrossRef](#)]
26. Jahangiri, A.; Rakha, H.A.; Dingus, T.A. Adopting Machine Learning Methods to Predict Red-light Running Violations. In Proceedings of the 2015 IEEE 18th International Conference on Intelligent Transportation Systems, Gran Canaria, Spain, 15–18 September 2015; pp. 650–655. [[CrossRef](#)]
27. Gates, T.J.; Savolainen, P.T.; Maria, H.-U. Prediction of Driver Action at Signalized Intersections by Using a Nested Logit Model. *Transp. Res. Rec. J. Transp. Res. Board* **2014**, *2463*, 10–15. [[CrossRef](#)]
28. Jahangiri, A.; Rakha, H.; Dingus, T.A. Red-light running violation prediction using observational and simulator data. *Accid. Anal. Prev.* **2016**, *96*, 316–328. [[CrossRef](#)]
29. Ren, Y.; Wang, Y.; Wu, X.; Yu, G.; Ding, C. Influential factors of red-light running at signalized intersection and prediction using a rare events logistic regression model. *Accid. Anal. Prev.* **2016**, *95*, 266–273. [[CrossRef](#)]
30. Hurwitz, D.S.; Wang, H.; Knodler, M.A.; Ni, D.; Moore, D. Fuzzy sets to describe driver behavior in the dilemma zone of high-speed signalized intersections. *Transp. Res. Part F Traffic Psychol. Behav.* **2012**, *15*, 132–143. [[CrossRef](#)]
31. Zaheri, D.; Abbas, M. An Algorithm for Identifying Red Light Runners from Radar Trajectory Data. In Proceedings of the 2015 IEEE 18th International Conference on Intelligent Transportation Systems-(ITSC 2015), Gran Canaria, Spain, 15–18 September 2015; pp. 2683–2687.
32. Zhang, L.; Wang, L.; Zhou, K.; Zhang, W.-B. Dynamic All-Red Extension at a Signalized Intersection: A Framework of Probabilistic Modeling and Performance Evaluation. *IEEE Trans. Intell. Transp. Syst.* **2011**, *13*, 166–179. [[CrossRef](#)]
33. Zyner, A.; Worrall, S.; Nebot, E. A Recurrent Neural Network Solution for Predicting Driver Intention at Unsignalized Intersections. *IEEE Robot. Autom. Lett.* **2018**, *3*, 1759–1764. [[CrossRef](#)]
34. Zyner, A.; Worrall, S.; Nebot, E. Naturalistic Driver Intention and Path Prediction Using Recurrent Neural Networks. *IEEE Trans. Intell. Transp. Syst.* **2019**, *21*, 1584–1594. [[CrossRef](#)]
35. Lee, E.H. Traffic Speed Prediction of Urban Road Network Based on High Importance Links Using XGB and SHAP. *IEEE Access* **2023**, *11*, 113217–113226. [[CrossRef](#)]
36. Kwak, K.; Lee, E.H. Impact of road transport system on groundwater quality inferred from explainable artificial intelligence (XAI). *Sci. Total Environ.* **2024**, *917*, 170388. [[CrossRef](#)] [[PubMed](#)]
37. Min, J.H.; Ham, S.W.; Kim, D.-K.; Lee, E.H. Deep Multimodal Learning for Traffic Speed Estimation Combining Dedicated Short-Range Communication and Vehicle Detection System Data. *Transp. Res. Rec. J. Transp. Res. Board* **2022**, *2677*, 247–259. [[CrossRef](#)]
38. Elhenawy, M.; Bond, A.; Rakotonirainy, A. C-ITS Safety Evaluation Methodology based on Cooperative Awareness Messages. In Proceedings of the 2018 21st International Conference on Intelligent Transportation Systems (ITSC), Maui, HI, USA, 4–7 November 2018; pp. 2471–2477.
39. Komol, M.R.; Elhenawy, M.; Masoud, M.; Glaser, S.; Rakotonirainy, A.; Wood, M.; Alderson, D. Deep Transfer Learning Based Intersection Trajectory Movement Classification for Big Connected Vehicle Data. *IEEE Access* **2021**, *9*, 141830–141842. [[CrossRef](#)]
40. Komol, M.M.R. C-ITS Based Prediction of Driver Red Light Running and Turning Behaviours. Master's Thesis, Queensland University of Technology, Brisbane City, Australia, 2022. Available online: <https://eprints.qut.edu.au/227694/> (accessed on 22 February 2022).
41. Akiba, T.; Sano, S.; Yanase, T.; Ohta, T.; Koyama, M. Optuna: A Next-generation Hyperparameter Optimization Framework. In Proceedings of the 25th ACM SIGKDD International Conference on Knowledge Discovery & Data Mining, Anchorage, AK, USA, 4–8 August 2019; pp. 2623–2631.

42. Smith, L.N. Cyclical learning rates for training neural networks. In Proceedings of the 2017 IEEE Winter Conference on Applications of Computer Vision (WACV), Santa Rosa, CA, USA, 24–31 March 2017; pp. 464–472. [[CrossRef](#)]
43. Prechelt, L. Early Stopping—But When? In *Neural Networks: Tricks of the Trade*, 2nd ed.; Montavon, G., Orr, G.B., Müller, K.-R., Eds.; Springer: Berlin/Heidelberg, Germany, 2012; pp. 53–67.

Disclaimer/Publisher’s Note: The statements, opinions and data contained in all publications are solely those of the individual author(s) and contributor(s) and not of MDPI and/or the editor(s). MDPI and/or the editor(s) disclaim responsibility for any injury to people or property resulting from any ideas, methods, instructions or products referred to in the content.